

Preparation and Characterization of Porous Chitosan-Tripolyphosphate Beads for Copper(II) Ion Adsorption

Shao-Jung Wu,¹ Tzong-Horng Liou,¹ Chao-Hsien Yeh,¹ Fwu-Long Mi,² Tsung-Kuan Lin³

¹Department of Chemical Engineering, Ming Chi University of Technology, New Taipei City 243, Taiwan, Republic of China

²Department of Biotechnology, Vanung University, Tao-Yuan Hsien 320, Taiwan, Republic of China

³Department of Applied Cosmetology, Hwa Hsia Institute of Technology, New Taipei City 235, Taiwan, Republic of China

Correspondence to: S.-J. Wu (E-mail: sjwu@mail.mcut.edu.tw)

ABSTRACT: Porous chitosan–tripolyphosphate beads, prepared by the ionotropic crosslinking and freeze-drying, were used for the adsorption of Cu(II) ion from aqueous solution. Batch studies, investigating bead adsorption capacity and adsorption isotherm for the Cu(II) ion, indicated that the Cu(II) ion adsorption equilibrium correlated well with Langmuir isotherm model. The maximum capacity for the adsorption of Cu(II) ion onto porous chitosan–tripolyphosphate beads, deduced from the use of the Langmuir isotherm equation, was 208.3 mg/g. The kinetics data were analyzed by pseudo-first, pseudo-second order kinetic, and intraparticle diffusion models. The experimental data fitted the pseudo-second order kinetic model well, indicating that chemical sorption is the rate-limiting step. The negative Gibbs free energy of adsorption indicated a spontaneous adsorption, while the positive enthalpy change indicated an endothermic adsorption process. This study explored the adsorption of Cu(II) ion onto porous chitosan–tripolyphosphate beads, and used SEM/EDS, TGA, and XRD to examine the properties of adsorbent. The use of porous chitosan–tripolyphosphate beads to adsorb Cu(II) ion produced better and faster results than were obtained for nonporous chitosan–tripolyphosphate beads. © 2012 Wiley Periodicals, Inc. *J. Appl. Polym. Sci.* 000: 000–000, 2012

KEYWORDS: adsorption; crosslinking; biopolymers and renewable polymers

Received 8 December 2010; accepted 16 May 2012; published online

DOI: 10.1002/app.38073

INTRODUCTION

The presence of heavy metal ions in water resources presents a huge problem for the environment due to their high toxicity. Conventional removal methods such as chemical precipitation, filtration, reverse osmosis, and ion exchange, are ineffective in removing trace levels of heavy metals from polluted aqueous solution.^{1–3} Liquid phase adsorption is an effective and extensively used method of removing heavy metal ions. Recently, workers have used biosorbents such as chitosan and its derivatives in the removal of low concentration heavy metal ions from wastewater.^{4,5} Chitosan derives from chitin, which is present in the shells of crustaceans, such as shrimps and crabs. Chitosan is hydrophilic, biocompatible, biodegradable, has antibacterial properties, and has a high adsorption capacity for heavy metals. It is well known the uptake of metal ion by chitosan is primarily influenced by coordination with the amino group. Furthermore, the amino groups of chitosan can react with hydrogen ions. Consequently, the two reactions compete during adsorption, and pH change leads to a change in the capacity for metal ion uptake. Since chitosan is susceptible to strong acid, it is nec-

essary to improve stability by introducing crosslinking. Crosslinking agents such as glutaraldehyde,^{6,7} epichlorohydrin,^{6,8} formaldehyde,⁹ and ethylene glycol diglycidyl ether^{6,10} are common, but are not ideal due to physiological toxicity effects. It has been reported that heavy metal ions could be effectively removed by pristine chitosan and chemically modified chitosan. A comparative study on the adsorption capacity of various adsorbents for Cu(II) ion was conducted. It was found that the Cu(II) ion adsorption capacity of zeolite was about 6.74 mg/g and 26 mg/g, respectively.^{11,12} The adsorption of Cu(II) ion on modified activated carbon was 38 mg/g.¹³ The adsorption of Cu(II) ion on dehydrated wheat bran was 51.5 mg/g.¹⁴ Removal of Cu(II) from aqueous solution by adsorption onto shells of lentil, wheat, and rice adsorbents was 9.588, 17.422, and 2.954 mg/g, respectively.¹⁵ The adsorption capacity of pristine chitosan was about 180 mg/g and 80 mg/g, respectively.^{2,6} The adsorption ability of chitosan usually reduces since some amino groups in chitosan chain are involved in crosslinking. For example, they are about 58 mg/g and 81 mg/g with glutaraldehyde modified chitosan.^{6,7} The second type of chemical modification is that the complexing agent is crosslinked with the $-\text{CH}_2\text{OH}$ groups of chitosan chain. The

adsorption capacity of Cu(II) ion on epichlorohydrin modified chitosan is about 62 mg/g.⁶ The adsorption capacity of chitosan for Cu(II) ion shows significant difference among the reports. The difference in chitosan adsorption capacity between the studies could be due to the difference of the analytical method, the source and composition, and the physical type of chitosan.

A novel and straightforward synthetic technique for the preparation of chitosan beads with less cytotoxicity is desirable. Chitosan has application in the preparation of nontoxic polyelectrolyte-complex products with polyanions. Chitosan forms gels with the nontoxic and multivalent tripolyphosphate counter ion.^{16–19} The ionic interactions between the positively charged amino groups and negatively charged counterion, tripolyphosphate, were used to prepare chitosan beads. The aim of this study was to develop nontoxic, porous chitosan–tripolyphosphate beads by ionotropic crosslinking and freeze-drying, for the adsorption of Cu(II) ion from aqueous solution. Langmuir and Freundlich isotherms were used to evaluate equilibrium adsorption data. The kinetics data were also determined based on the pseudo-first order, pseudo-second order, and intraparticle diffusion equations. Additionally, thermodynamic parameters for the adsorption of Cu(II) ion by the porous chitosan–tripolyphosphate beads were also studied. This article includes a comparison of the adsorption properties of porous and nonporous chitosan–tripolyphosphate beads, and the results for the application of porous chitosan–tripolyphosphate beads are evaluated in future wastewater treatments.

EXPERIMENTAL

Materials

Chitosan ($M_w \sim 400,000$, 98% deacetylated) was purchased from Charming & Beauty (Taiwan). Sodium tripolyphosphate and copper (II) sulfate pentahydrate were purchased from Showa. Other materials were reagent grade. Deionized (DI) water was used throughout the study.

Preparation of Porous Chitosan–Tripolyphosphate Beads

Chitosan (2 g) was dissolved in acetic acid solution (100 mL, 1% v/v) to prepare the chitosan solution. The chitosan solution was added dropwise into a gently agitated tripolyphosphate solution (7.5% w/v) through precision tubing with inner diameter of 0.8 mm using a tubing pump. The gelled beads formed instantly as the chitosan solution contacted the tripolyphosphate solution. The solidified beads were kept in the solution for 12 h prior to filtration and thorough rinsing with DI water. The beads were then preheated in an oven at 35°C for 1 h, followed by freeze-drying (Eyela, freeze dryer FDU-2100) to produce porous chitosan–tripolyphosphate beads. The freezing temperature is -77°C . The particle size of the porous beads was about 1.5 mm. Drying the beads at 35°C for 24 h provided nonporous chitosan–tripolyphosphate beads, and the size of the nonporous beads was about 1 mm.

Scanning Electron Microscopy with Energy Dispersive Spectrometry Analysis

Porous and nonporous chitosan–tripolyphosphate beads were coated with a thin gold layer using the Hitachi IB-2 coating unit. Coated samples were examined using a Hitachi S-2300

scanning electron microscope. The copper distribution on the cross-section of porous and nonporous beads was analyzed by the energy dispersive spectrometer (EDS) (Link, AN-10000).

Thermogravimetric Analysis

TGA was performed with a METTLER TGA/SDTA851 analyzer. The mass of each sample was about 5 mg. Nitrogen was used as purge gas with a flow rate of 60 mL/min. The samples were heated from 30°C to 500°C at a heating rate of 10°C/min to record the TG curves.

X-Ray Diffraction

The XRD patterns of pristine chitosan, porous and nonporous chitosan–tripolyphosphate beads were recorded on an x-ray diffractometer (PANalytical, model X'pert pro system). The samples were irradiated with monochromatized Cu K α radiation (0.154 nm) and analyzed between 4 and 50° (2θ). The voltage and current used were 45 kV and 40 mA, respectively.

Adsorption Experiments

A Cu(II) ion stock solution (3000 mg/L) was prepared by dissolving copper(II) sulfate pentahydrate in DI water. The stock solution was diluted as necessary to provide appropriate concentrations for adsorption studies. Batch adsorption experiments were conducted in 1000-mL beakers with 1000-mL standard solutions and equilibrated using 1 g porous or nonporous chitosan–tripolyphosphate beads at 100 rpm (25°C). The initial pH in various Cu(II) ion concentrations (100–3000 mg/L) for adsorption studies was between 5.3 and 4.7. According to Lee et al.,¹⁷ the best working pH value of chitosan–tripolyphosphate beads for Cu(II) ion adsorption is about 5. The chitosan adsorbent exhibited a drastic decrease in Cu(II) ion affinity at low pH conditions due to formidable competition with hydronium ions. Wan Ngah and Fatimathan also stated that the adsorption capacity for Cu(II) ion was very low at lower pH.¹⁹ So the initial pH of the Cu(II) ion aqueous solution were adjusted at pH 5 using appropriate concentrations of HCl or NaOH solutions throughout the study. The effect of temperature on porous bead adsorption capacity was studied at Cu(II) ion solution (1000 mL, 50 mg/L) temperatures of 30, 40, 50, and 60°C. For each study temperature, the system was allowed to equilibrate with 1 g of porous chitosan–tripolyphosphate beads. Adsorption kinetics was studied using an initial concentration of 100 mg/L with the adsorbent dosage of 1 g/1000 mL at pH 5. The Cu(II) ion concentration determined at intervals using inductively coupled plasma-optical emission spectrometer (ICP-OES, Perkin Elmer Optima 200DV). All samples were filtered by syringe filters, with pore size 0.45 μm , prior to ICP-OES measurement. The adsorption was calculated by:

$$Q = [V \times (C_o - C_t)]/W \quad (1)$$

where C_o (mg Cu(II)/L) and C_t (mg Cu(II)/L) are the initial Cu(II) ion concentration and the sampled Cu(II) ion concentration at time t , V is the volume of solution (L), W is the mass of beads (g), and Q is the adsorption capacity of Cu(II) ion on the beads (mg Cu(II)/g chitosan–tripolyphosphate beads). For each test run, the average of three replicates was reported.

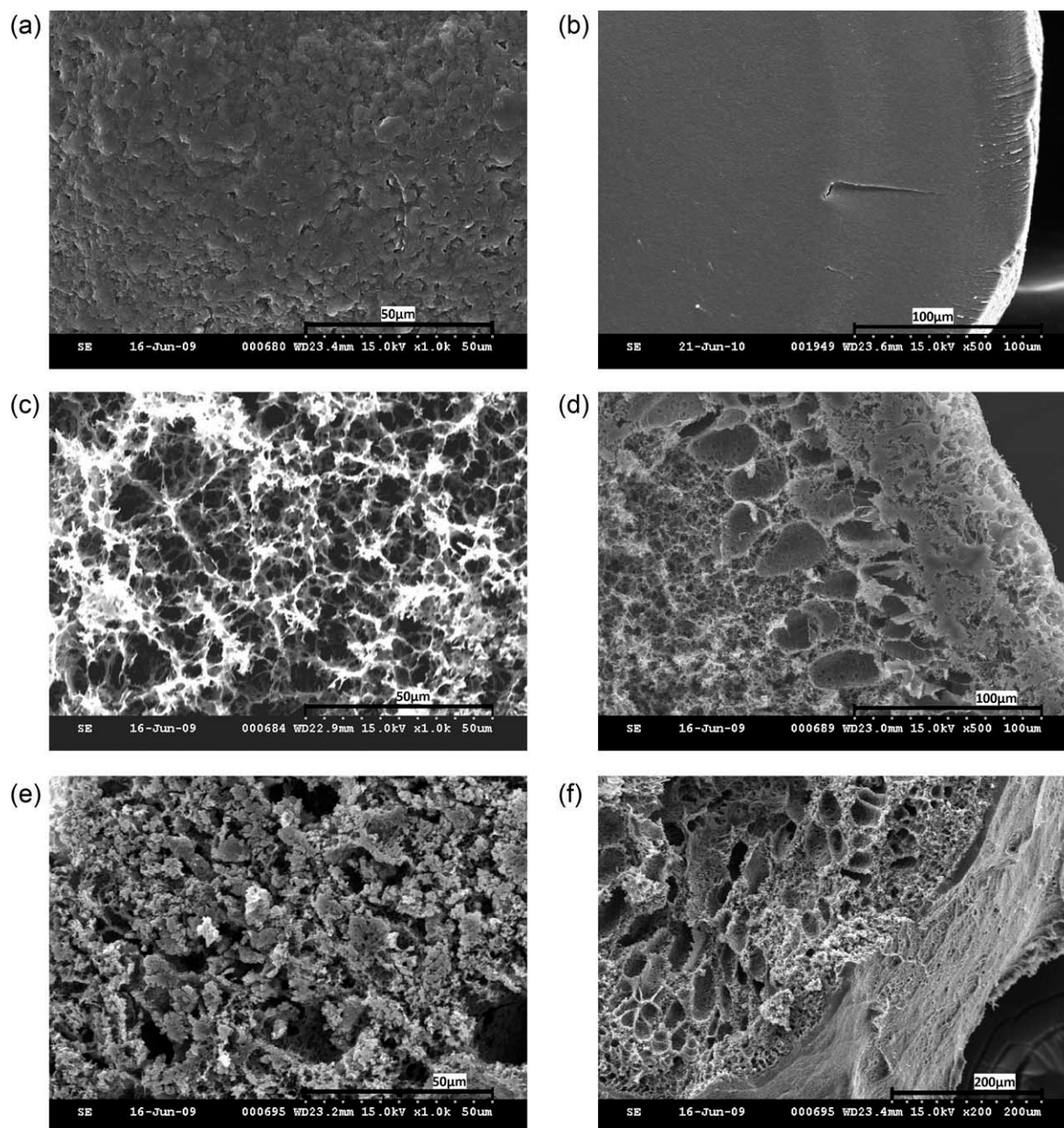


Figure 1. SEM micrographs: (a) the surface of nonporous chitosan–tripolyphosphate bead, (b) the cross-section of nonporous chitosan–tripolyphosphate bead, (c) the surface of porous chitosan–tripolyphosphate bead, (d) the cross-section of porous chitosan–tripolyphosphate bead, (e) the surface of Cu(II) ion adsorbed porous chitosan–tripolyphosphate bead, (f) the cross-section of Cu(II) ion adsorbed porous chitosan–tripolyphosphate bead.

RESULTS AND DISCUSSION

Morphology of Porous and Nonporous Chitosan–Tripolyphosphate Beads

The surface of prepared chitosan–tripolyphosphate beads was examined by SEM. Figure 1(a, b) shows the morphology of nonporous chitosan–tripolyphosphate beads without freeze-drying, both the surface and cross-section appear dense. Thus, it is difficult to obtain the BET surface area of the nonporous beads. As can be seen from Figure 1(c), honeycombed pores (pore size 1–10 μm) form on the surface of freeze-dried chitosan–tripolyphosphate beads. The BET surface area of the porous beads is

approximately 6.40 m^2/g . Figure 1(d) shows that the cross-section of freeze-dried chitosan–tripolyphosphate beads is also porous, although density is greater near the bead surface, compared with the center of the beads, where pores are more numerous. This dense surface structure greatly enhances the mechanical properties of the porous beads during the adsorption process. SEM images for porous chitosan–tripolyphosphate beads before and after adsorption of Cu(II) ion showed that the surface and cross-sectional morphology changed considerably during the adsorption process. Following Cu(II) ion adsorption [Figure 1(e)], the surface morphology shows copper-like

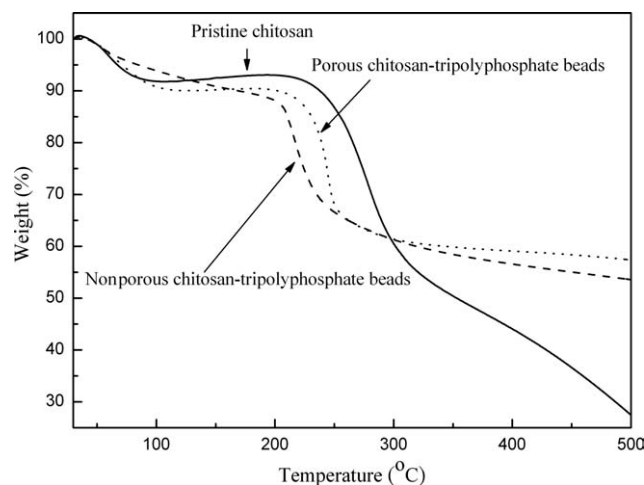


Figure 2. TGA curves of pristine chitosan, porous and nonporous chitosan–tripolyphosphate beads.

particles deposited on the surface, while the cross-section structure contains fewer voids, and appears denser than before adsorption [Figure 1(f)].

Materials Characterization

TGA curves of pristine chitosan, porous, and nonporous chitosan–tripolyphosphate beads show a weight loss in two stages shown in Figure 2. For pristine chitosan the first stage of weight loss is about 8% in between 50 and 120°C. This may be due to the loss of adsorbed and bound water. The second stage starts at 253°C and the fastest decomposition rate temperature is 276°C. At 500°C 70% weight loss happens due to degradation of chitosan. For the porous chitosan–tripolyphosphate beads the degradation behavior is different from pristine chitosan. Here the first stage of weight loss is due to the removal of water content. The onset degradation temperature starts earlier at around 233°C and the fastest decomposition rate temperature decreases to 244°C. The result means that the different arrangements of the molecular chains in the structure with higher amorphous domains for the porous chitosan–tripolyphosphate beads. But the porous chitosan–tripolyphosphate beads gain greater thermal stability than the pristine chitosan in the temperature range of 300 and 500°C. The higher stability is due to the presence of inorganic tripolyphosphate in the crosslinked backbones. For the nonporous chitosan–tripolyphosphate beads the degradation behavior is somewhat like porous chitosan–tripolyphosphate beads. At the first stage, the weight loss of the nonporous chitosan–tripolyphosphate beads is lower than that of the porous chitosan–tripolyphosphate beads. There might be more water adsorbed on the porous chitosan–tripolyphosphate beads.

Crystallographic structure of pristine chitosan, porous, and nonporous chitosan–tripolyphosphate beads were determined by XRD shown in Figure 3. There are two prominent peaks at 12° (2θ) and 20° (2θ) of pristine chitosan, indicating the high degree of crystallinity of chitosan. However, in the case of crosslinked chitosan there is significant decrease in the intensity of characteristic peaks of porous and nonporous chitosan–tripolyphosphate beads, indicating the characteristic of an amorphous structure.

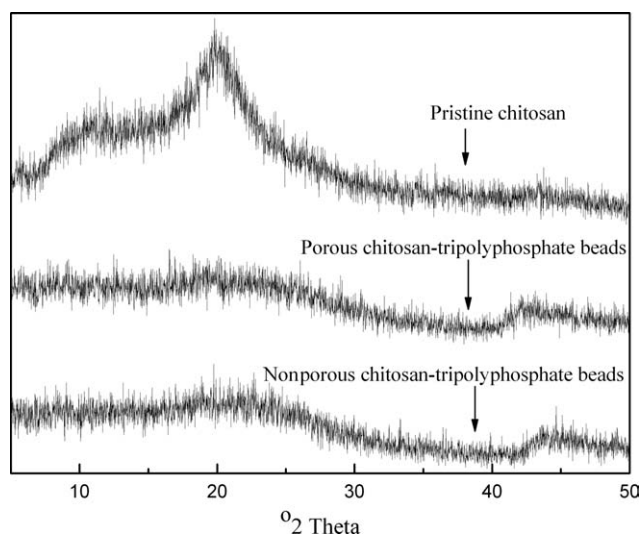


Figure 3. XRD patterns of pristine chitosan, porous and nonporous chitosan–tripolyphosphate beads.

Effect of Contact Time

Figure 4 shows the effect of contact time on Cu(II) ion retention capacity for porous and nonporous chitosan–tripolyphosphate beads. The contact time varied in the range 0–120 h, with the initial Cu(II) ion concentration fixed at 300 mg/L. Dosage of chitosan beads was held at 1 g/L. From Figure 4, it shows that 24 h contact at 100 rpm could achieve equilibrium for porous beads, whereas nonporous beads require longer contact times (72 h) to achieve equilibrium. The adsorption of Cu(II) ion by porous chitosan–tripolyphosphate beads was faster compared to nonporous beads. The difference in equilibration time is due to the porous structure of the freeze-dried beads. EDS was used for analyzing the distribution of Cu(II) ions on the cross-section of the beads. A small amount of copper on the cross-section of the porous chitosan–tripolyphosphate beads is detected after a contact time of 60 min, which indicates that Cu(II) ion has diffused inside the porous beads. For the

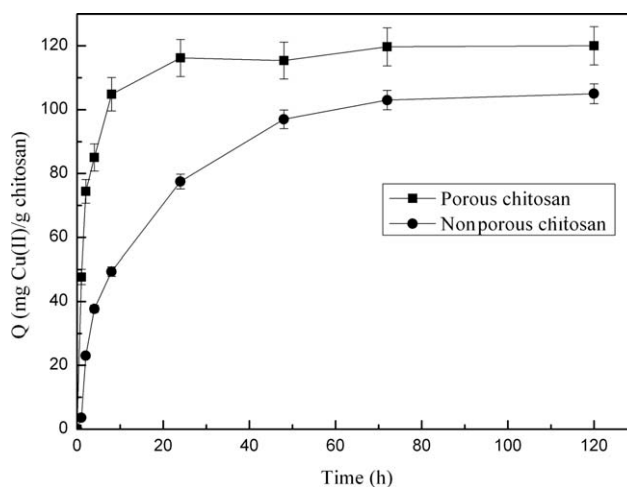


Figure 4. Effect of contact time on the adsorption of Cu(II) ion onto porous and nonporous chitosan–tripolyphosphate beads.

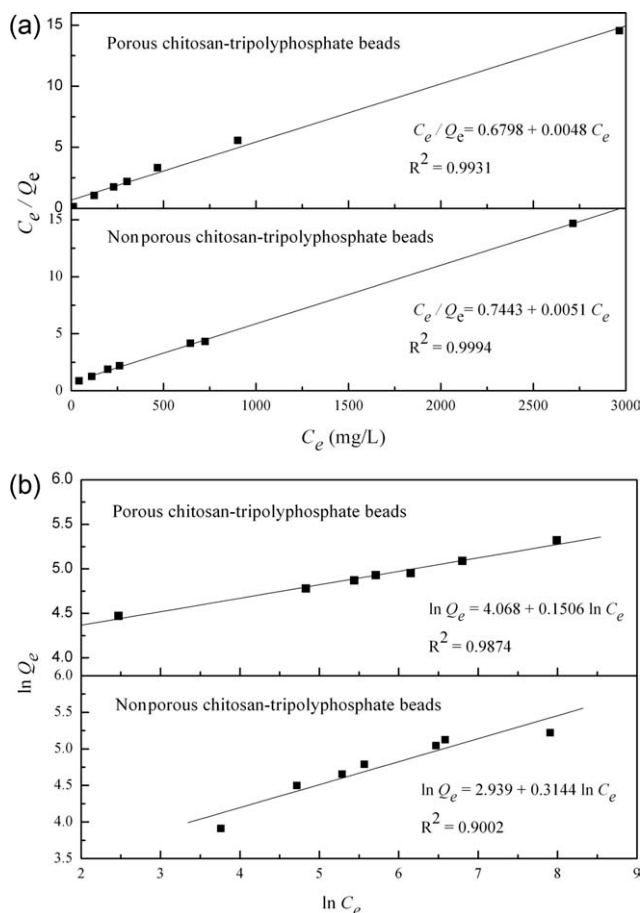


Figure 5. The results of fitting experimental data of Cu(II) ion onto porous and nonporous chitosan-tripolyphosphate beads to (a) Langmuir isotherm and (b) Freundlich isotherm.

nonporous beads required up to 8 hours for diffusion of Cu(II) ion inside them. The Cu(II) ion adsorption capacity of porous chitosan-tripolyphosphate beads was 120 mg/g, while nonporous chitosan-tripolyphosphate beads had a capacity of around 105 mg/g.

Adsorption Isotherms

Isotherms can illustrate the equilibrium characteristics of the adsorption of Cu(II) ion onto porous and nonporous chitosan-tripolyphosphate beads, and so describe the adsorption behaviors between adsorbate and adsorbent. The adsorption capacity increases with initial concentration of Cu(II) ion, and tends to equilibrium in 24 h for porous chitosan-tripolyphosphate beads and in 72 h for nonporous chitosan-tripolyphosphate beads. The relationship between adsorption capacity and concentration of Cu(II) ion in solution is described by two models set out below.²⁰

The nonlinear form of the Langmuir isotherm is expressed as follows:

$$Q_e = \frac{Q_m K_L C_e}{1 + K_L C_e} \quad (2)$$

where Q_e is the amount of metal ions adsorbed per mass unit of adsorbent at equilibrium (mg/g), C_e is the concentration of

remaining metal ions in solution at equilibrium (mg/L), Q_m is the saturated adsorption capacity of metal ions per mass unit of adsorbent (mg/g), and K_L is the Langmuir adsorption constant related to binding site affinity (L/mg). The values of K_L and Q_m are determined from the intercept and slope of the plot of (C_e/Q_e) vs. C_e using the linear form of eq. (2). The Langmuir isotherm model characterizes adsorption occurring at specific homogeneous adsorption sites within the adsorbent. Furthermore, it assumes that the adsorption occurs within a single molecular layer, and is distributed evenly at adsorption sites. Maximum adsorption occurs when adsorbed molecules on the surface of the adsorbent form a saturated layer. All adsorption sites involved are energetically identical and intermolecular forces decreases with distance from the adsorption surface.

The Freundlich isotherm is an empirical equation, characterizing adsorption on uneven surfaces.²¹ It is suitable for high and medium concentrations, but is unsuitable for low concentration samples. The nonlinear Freundlich isotherm is expressed as follows:

$$Q_e = K_F C_e^{1/n} \quad (3)$$

where Q_e is the amount of metal ions adsorbed per mass unit adsorbent at equilibrium (mg/g), C_e is the concentration of metal ions remaining in solution at equilibrium (mg/L). K_F (mg/g) and n are Freundlich constants, which characterize adsorption capacity (mg/g) and intensity respectively. A plot of linearized $\ln Q_e$ vs. $\ln C_e$ enables the constant K_F and exponent $1/n$ to be determined.

Figures 5(a, b) show the results of fitting experimental data to Langmuir and Freundlich isotherms, respectively. The straight line plots of Langmuir and Freundlich isotherm models indicate that the adsorption of Cu(II) ion on porous and nonporous chitosan-tripolyphosphate beads follows both Langmuir and Freundlich isotherms. Table I provides calculated results for the Langmuir and Freundlich isotherms. The higher value of correlation coefficient (R^2) for Langmuir than for Freundlich isotherm indicates that the adsorption data provided better fit in Langmuir isotherm model. The Langmuir isotherm would be the predominant adsorption process involved in the overall

Table I. Isotherm Constants for Adsorption of Cu(II) ion Onto Porous and Nonporous Chitosan-Tripolyphosphate Beads

Adsorption model	Cu(II) ion	
	Porous beads	Nonporous beads
Langmuir isotherm		
Q_m (mg/g)	208.3	196.1
K_L (L/mg)	0.0071	0.0069
R^2	0.9931	0.9994
Freundlich isotherm		
n	6.640	3.181
K_F (mg/g)	58.44	18.90
R^2	0.9874	0.9002

Table II. Kinetic Parameters for the Adsorption of Cu(II) Ion Onto Porous and Nonporous Chitosan–Tripolyphosphate Beads

kinetic equation	Cu(II) ion	
	Porous beads	Nonporous beads
$Q_{e(\text{exp.})}(\text{mg/g})$	87.28	50.02
Pseudo-first order constant		
$K_1(\text{min}^{-1})$	1.20×10^{-3}	4.20×10^{-4}
$Q_{e(\text{theor.})}(\text{mg/g})$	54.92	33.69
R^2	0.9549	0.9273
Pseudo-second order constant		
$K_2(\text{g/mg} \cdot \text{min})$	7.04×10^{-5}	7.15×10^{-7}
$Q_{e(\text{theor.})}(\text{mg/g})$	90.09	50.76
R^2	0.9999	0.9969
Intraparticle diffusion constants		
$k_{i,1}(\text{mg/g min}^{1/2})$	2.522	1.830
R^2	0.9815	0.9998
$k_{i,2}(\text{mg/g min}^{1/2})$	0.248	0.215
R^2	0.9685	0.9764

adsorption process for porous and non porous chitosan–tripolyphosphate beads. According to the Langmuir isotherm, the maximum theoretical Cu(II) ion adsorption capacity is higher for porous chitosan–tripolyphosphate beads (208.3 mg/g) than nonporous chitosan–tripolyphosphate beads (196.1 mg/g). The Freundlich isotherm, predicts n , representing adsorption favorability, as greater than one, indicating that adsorption intensity is favorable at high concentrations.

Adsorption Kinetics

Kinetic models were used to determine the adsorption kinetics and rate-limiting step for the adsorption of Cu(II) ion by porous and nonporous chitosan–tripolyphosphate beads. The experimental data obtained using Cu(II) ion solution with concentration of 100 mg/L. Dosage of the adsorbent was fixed at 1 g/L. The rate of Cu(II) ion adsorption by porous beads was determined using three different kinetic analyses. The first analysis used the pseudo-first order equation of Lagergren:²²

$$\ln(Q_e - Q_t) = \ln Q_e - k_1 t \quad (4)$$

where Q_e and Q_t are the amounts of Cu(II) ion adsorbed onto adsorbent (mg/g) at equilibrium and at time t , respectively. The k_1 parameter is the rate constant for first-order adsorption (min^{-1}). Linear plots of $\ln(Q_e - Q_t)$ against t were used to determine the rate constant, k_1 , and the correlation coefficient, R^2 .

The pseudo-second order kinetics can be expressed by:²³

$$\frac{t}{Q_t} = \frac{1}{k_2 Q_e^2} + \frac{t}{Q_e} \quad (5)$$

where Q_e and Q_t are the amounts of Cu(II) ion adsorbed onto adsorbent (mg/g) at equilibrium and at time t , and k_2 is the adsorption rate constant for second-order adsorption (g/mg

min). Linear plots of t/Q_t against t were used to determine the rate constant, k_2 and the correlation coefficient, R^2 .

Table II summarizes adsorption kinetic parameters. The theoretical Q_e value, estimated from the pseudo-first order kinetic model, is significantly different from the experimentally determined value, furthermore, the correlation coefficient (R^2) is much less than 1.0, while for the pseudo-second order kinetic model, the correlation coefficient (R^2) is greater than 0.99. These correlation results suggest that the adsorption of Cu (II) ion onto porous and nonporous chitosan–tripolyphosphate beads exhibits pseudo-second order kinetics. Moreover, the calculated equilibrium adsorption capacity values, Q_e (theor.) are very close to the experimental Q_e (exp.) values for both porous and nonporous chitosan–tripolyphosphate beads. Therefore, it is reasonable to conclude that the rate-limiting step in the adsorption of Cu(II) ion onto porous and nonporous chitosan–tripolyphosphate beads is chemisorption involving sharing or exchange of electrons between the Cu(II) ion and the chitosan.²⁴

The pseudo-first and second-order equations only predict the behavior over the whole range of adsorption, the present finding does not confirm any particular adsorption mechanism. In order to propose a reasonable diffusion process for the adsorption of Cu(II) ion onto porous and nonporous chitosan–tripolyphosphate beads, we integrated the intraparticle diffusion model.²⁵ The intraparticle diffusion rate constant k_i ($\text{mg/g min}^{1/2}$) was determined by linearization of the curve $Q_t = f(t^{0.5})$.

$$Q_t = k_i t^{0.5} \quad (6)$$

The adsorption process on a porous adsorbent is mainly controlled by four steps. These steps involve bulk diffusion, film diffusion, intraparticle diffusion, and finally uptake of Cu(II) ion on the active sites. The experimental data obtained for 100 mg/L of Cu(II) ion solution were plotted in terms of the parameters mentioned above. Dosage of the porous beads was fixed at 1 g/L. Figure 6 shows two interdependent linear lines indicated two steps in the adsorption kinetics. Since the experiment was conducted with stirring, effect of bulk diffusion could

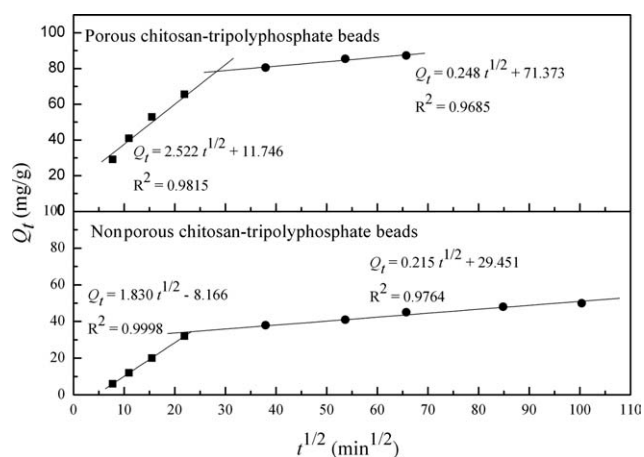


Figure 6. Intraparticle diffusion model fitted for the adsorption of Cu(II) ion onto porous and nonporous chitosan–tripolyphosphate beads.

Table III. Thermodynamic Parameters for the Adsorption of Cu(II) Ion Onto Porous and Nonporous Chitosan–Tripolyphosphate Beads

	ΔG° (kJ/mol)				ΔH° (kJ/mol)	ΔS° (J/mol K)
	30°C	40°C	50°C	60°C		
Porous beads	-8.90	-10.97	-12.86	-15.76	13.08	53.67
Nonporous beads	-0.191	-1.138	-2.142	-2.851	27.08	90.12

be neglected. Further, the intraparticle diffusion of Cu(II) ion into nonporous chitosan–tripolyphosphate beads would be slower than that of porous chitosan–tripolyphosphate beads. The EDS analysis of copper distribution on the cross-section of the nonporous chitosan–tripolyphosphate beads displayed no signal of copper ion before the first 8 h. So the first, the steeper line of nonporous chitosan–tripolyphosphate beads is the film diffusion step ($Q = 1.830 t^{1/2} - 8.166$), and the second, the gradual line is the intraparticle diffusion step ($Q = 0.215 t^{1/2} + 29.451$). The intraparticle diffusion of Cu(II) ion into glassy state nonporous chitosan–tripolyphosphate beads is slow due to lower hydration of the beads. For the porous chitosan–tripolyphosphate beads, the EDS analysis indicates that after a contact time of 1 hour, Cu(II) ion has diffused inside the beads. So the first linear slope represents intraparticle diffusion, while the plateau corresponds to the equilibrium state. The slope of each stage is termed as the rate parameter $k_{i,1}$ and $k_{i,2}$, as detailed in Table III. The straight line does not pass through the origin, indicating that intraparticle transport is not the rate-limiting step in the adsorption process of Cu(II) ion onto porous chitosan–tripolyphosphate beads.²⁶

Thermodynamics of Cu(II) Ion Adsorption

To determine the thermodynamic parameters of Cu(II) ion adsorption onto porous and nonporous chitosan–tripolyphosphate beads, the adsorption experiments were performed at four different temperatures (30, 40, 50, and 60°C) under 50 mg/L of Cu(II) ion solution. Dosage of the adsorbent was fixed at 1 g/L. The equilibrium constant for adsorption, K_C , for Cu(II) ions was calculated using eq. (7).²⁷

$$K_C = X_e / (C_i - X_e) \quad (7)$$

where X_e is the concentration of solute adsorbed on the resin at equilibrium, mg/L, C_i is the initial ion concentration, mg/L. The adsorption capacity of porous chitosan–tripolyphosphate beads shows an increment from 39.95 mg/g at 30°C to 43.90 mg/g at 60°C. The observed increase in adsorption capacity with temperature was in accord with literature reports.^{19,28} This temperature dependence allowed us to use K_C values to predict the Gibbs free energy change (ΔG°), enthalpy change (ΔH°), and entropy change (ΔS°). These thermodynamic parameters were calculated by using the following relationships:

$$\Delta G^\circ = -RT \ln K_C \quad (8)$$

$$\ln K_C = -\frac{\Delta H^\circ}{RT} + \frac{\Delta S^\circ}{R} \quad (9)$$

where R is the gas constant (8.314 J/mol K) and T is the temperature in Kelvin. Table III shows values for ΔH° and ΔS° cal-

culated from the slope and intercept of the plot of $\ln K_C$ vs. $1/T$. The correlation coefficient, R^2 , obtained for Cu(II) ion, is more than 0.99. The negative values of ΔG° indicate that the adsorption process is both thermodynamically favorable, and spontaneous for porous and nonporous chitosan–tripolyphosphate beads in the temperature range 30–60°C. The increasingly negative value of ΔG° as temperature increases means a greater driving force for adsorption at high temperatures.²⁹ The positive ΔH° value for the adsorption of Cu(II) ion, means that adsorption is an endothermic process. The positive value of ΔS° shows an irregular increase in randomness occurs at the bead-solution interface during adsorption.¹⁹ These thermodynamic parameters are the actual indicators for the practical applicability of an adsorption process.

CONCLUSIONS

Equilibrium adsorption experiments showed that porous chitosan–tripolyphosphate beads are an effective adsorbent for the removal of Cu(II) ion. The Langmuir isotherms fitted well with our adsorption equilibrium data. Adsorption of Cu(II) ion onto porous chitosan–tripolyphosphate beads followed a pseudo-second order mechanism, with chemisorption as the rate-limiting step. The thermodynamic parameters indicate that the adsorption process is spontaneous, and becomes more favorable at higher temperature. The adsorption of Cu(II) ion by porous chitosan–tripolyphosphate beads occurred at a higher rate compared with nonporous beads, and showed greater adsorption capacity for the target ions.

ACKNOWLEDGMENTS

The financial support of this research by the NSC of R.O.C., project No. 95-2221-E-131-018 is gratefully acknowledged.

REFERENCES

- Jung, R. S.; Shao, H. J. *Adsorption* **2002**, *8*, 71.
- Ng, J. C. Y.; Cheung, W. H.; McKay, G. J. *Colloid Interface Sci.* **2002**, *255*, 64.
- Li, N.; Bai, R. *Sep. Purif. Technol.* **2005**, *42*, 237.
- Guibal, E. *Sep. Purif. Technol.* **2004**, *38*, 43.
- Wu, F. C.; Tseng, R. L.; Juang, R. S. *J. Environ. Manage.* **2010**, *91*, 798.
- Wan Ngah, W. S.; Endud, C. S.; Mayanar, R. *React. Funct. Polym.* **2002**, *50*, 181.
- Juang, R. S.; Wu, F. C.; Tseng, R. L. *Bioresour. Technol.* **2001**, *80*, 187.
- Ge, H.; Huang, S. J. *Appl. Polym. Sci.* **2010**, *115*, 514.

9. Du, W. L.; Niu, S. S.; Xu, Z. R.; Xu, Y. L. *J. Appl. Polym. Sci.* **2009**, *111*, 2881.
10. Kamaril, A.; Wan Ngah, W. S.; Liew, L. K. *J. Environ. Sci.* **2009**, *21*, 296.
11. Panayotova, M. I. *Waste Manage.* **2001**, *21*, 671.
12. Perić, J.; Trgo, M.; Vukojević Medvidović, N. *Water Res.* **2004**, *38*, 1893.
13. Monser, L.; Adhoum, N. *Sep. Purif. Technol.* **2002**, *26*, 137.
14. Özer, A.; Özer, D.; Özer, A. *Process Biochem.* **2004**, *39*, 2183.
15. Aydın, H.; Bulut, Y.; Yerlikaya, Ç. *J. Environ. Manage.* **2008**, *87*, 37.
16. Mi, F. L.; Shyu, S. S.; Kuan, C. Y.; Lee, S. T.; Lu, K. T.; Jang, S. F. *J. Appl. Polym. Sci.* **1999**, *74*, 1868.
17. Lee, S. T.; Mi, F. L.; Shen, Y. J.; Shyu, S. S. *Polymer* **2001**, *42*, 1879.
18. Wu, S. J.; Liou, T. H.; Mi, F. L. *Bioresour. Technol.* **2009**, *100*, 4348.
19. Wan Ngah, W. S.; Fatinathan, S. J. *Environ. Manage.* **2010**, *91*, 958.
20. Frank, L. S. *Adsorption Technology: A Step-by-Step Approach to Evaluation and Application*; Marcel Dekker: New York, **1985**.
21. Hasan, M.; Ahmad, A. L.; Hameed, B. H. *Chem. Eng. J.* **2008**, *136*, 164.
22. Annadurai, G.; Krishnan, M. R. V. *Indian J. Chem. Technol.* **1997**, *4*, 213.
23. Mckay, G.; Ho, Y. S. *Water Res.* **1999**, *33*, 578.
24. Septhum, C.; Rattanaphani, S.; Bremner, J. B.; Rattanaphani, V. J. *Hazard. Mater.* **2007**, *148*, 185.
25. Wu, F. C.; Tseng, R. L.; Juang, R. S. *J. Hazard. Mater.* **2000**, *B73*, 63.
26. Özcan, A.; Öncü, E. M.; Özcan, A. S. *Colloids Surf. A-Physicochem. Eng. Asp.* **2006**, *277*, 90.
27. Dinu, M. V.; Dragan, E. S. *Chem. Eng. J.* **2010**, *160*, 157.
28. Kannamba, B.; Reddy, K. L.; AppaRao, B. V. *J. Hazard. Mater.* **2010**, *175*, 939.
29. Crini, G.; Badot, P. M. *Prog. Polym. Sci.* **2008**, *33*, 399.